Mesomorphic glass-forming ionic complexes composed of a cholesterol phthalate and 1-C*n*-3-methylimidazolium: phase transition and enthalpy relaxation behavior

Itaru Nakajima[1] · Taishi Kitaguchi[1] · Kazuki Sugimura[1] · Yoshikuni Teramoto [ID][2] · Yoshiyuki Nishio [ID][1]

Abstract

Ionic complexes consisting of a mesogenic cholesterol derivative and 1-alkyl (C*n*)-3-methylimidazolium (C*n*Mim) ($n =$ 6–18) were prepared from ethanol solutions containing an equimolar mixture of cholesterol hydrogen phthalate (CHP) and 1-C*n*-3-methylimidazolium hydroxide; the imidazolium hydroxide was obtained by anion exchange of 1-C*n*-3-methylimidazolium bromide. The complex samples, termed [C*n*Mim][CHP], were examined to evaluate their thermal transition patterns. Excluding the two samples ($n =$ 6, 8) that showed no definite ordered phase, the complexes with $n \geq 10$ formed a cholesteric ($n =$ 10, 12) or smectic ($n =$ 14–18) mesophase in a considerably wide range of temperatures; this wide range reflects the additional thermotropic property of the salts of C*n*Mim with longer alkyl chains. These fluid mesophases transformed into a mesomorphic vitreous solid without crystallization in a usual cooling process. For the glassy mesomorphic samples of selected complexes ($n =$ 10, 18), the enthalpy relaxation behavior was followed as a function of the aging temperature and time, and the data were analyzed in terms of a Kohlrausch–Williams–Watts (KWW) type of stretched exponential equation. A very narrow distribution of relaxation times was observed for the "liquid crystalline glasses", indicating the high uniformity of the relaxation mode.

Introduction

Liquid crystalline (LC) compounds of low molecular weight, which show a generally low melt viscosity, minimally vitrify, and easily crystallize in a cooling process from their mesomorphic molten state. However, when the molecular weight of the LC compound is increased to ca. 500–2000 g mol^{-1} via modification to form a branched structure and/or multiple mesogenic moieties, the products with medium molecular weights often form a glassy LC phase [1–5] as a result of suppression of the

crystallizability. Such mesomorphic glass-forming compounds can be applied as optical films or core elements in displays [6] and other information materials [3, 7] owing to their temperature-dependent properties of coloration or light transmittance. For example, vitrifiable LC compounds are promising for application as a rewritable recording medium, viz., some information can be transferred mechanically, electrically, or photochemically to a mesophase at a temperature above the glass transition temperature (T_g), and by simple cooling, the information can be stored in the glassy state. The stored information can be erased, for instance, by isotropization at high temperatures, and then a second set of information can be written in the same cycle. The vitrification phenomenon also prevails in LC polymers of higher molecular weight, and these polymers are usable as various optical media for storing information; however, it is usually difficult to obtain a fast and uniform response of the mesomorphic assembly to external stimuli, which is principally due to the high melt viscosity of the polymers.

In an earlier study [8], one of the authors (YN) successfully synthesized moderate molecular weight compounds that formed a glassy LC phase without complicated and time-consuming procedures by a simple mixing and

✉ Yoshiyuki Nishio
ynishio@kais.kyoto-u.ac.jp

[1] Division of Forest and Biomaterials Science, Graduate School of Agriculture, Kyoto University, Kyoto 606-8502, Japan

[2] Department of Applied Life Science, Faculty of Applied Biological Sciences, Gifu University, Gifu 501-1193, Japan

solvent evaporation method. Those compounds were actually stoichiometric 1:1 complex salts composed of a cholesterol ester/aliphatic amine pair, where cholesterol hydrogen phthalate (CHP) and cholesterol hydrogen succinate (CHS) were used as the cholesterol derivative component and a series of normal alkyl amines (Cn-amine, n (carbon number) = 12–18) were employed as the aliphatic amine component. The structural formulae of the constituents are shown in Fig. 1. As indicated in this figure, the complexes were stabilized by ionic interactions through salt formation between the carboxylic acid of CHP (or CHS) and the amino group of Cn-amine. After the study of the thermotropic phase behavior of the complexes, we next investigated the so-called enthalpy relaxation phenomenon resulting from physical aging of vitreous solids by using the "LC glasses" of the CHP/Cn-amine complexes, each of which had a defined molecular weight (≤800) [9, 10]. It was observed that the distribution of the relaxation times of the CHP/Cn-amine glasses was much narrower than that of conventional amorphous polymer glasses.

In extension of the above studies, we recently undertook a comparative study using similar cholesterol-based complexes prepared by altering the ionic ingredients to identify a general trend in the thermal properties and suggest a practical functionality for this kind of complex material. In the present work, the previous cation component (i.e., Cn-amine) was replaced with a 1-normal alkyl (Cn)-3-methylimidazolium cation, [CnMim]$^+$, to produce an ionic complex, [CnMim][CHP] (see Fig. 1). This cation is known as a representative component of ionic liquids (ILs), which have attracted a gr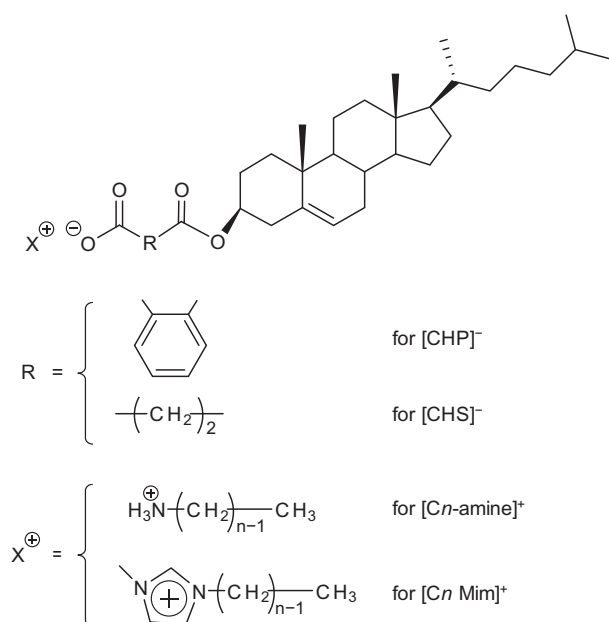eat deal of attention not only as green solvents [11, 12] but also as a new component of ion conductive materials [13]. Mesomorphic ILs that are capable of forming an LC phase have also been extensively studied in past decades [14–16]. As an advanced example of materialization, a one-dimensional ion conductive material was successfully designed by using ILs that formed a columnar LC phase [17, 18].

In this paper, we demonstrate the preparation of a new LC glass-forming complex material in which the core of familiar ILs, N-substituted imidazolium, is incorporated. The thermotropic phase transition and enthalpy relaxation behavior of the [CnMim][CHP] complexes are characterized with particular attention to the dependence on the Cn length of the imidazolium component.

Materials and methods

Original materials

CHP was purchased from Tokyo Chemical Industry (Tokyo, Japan) and used after purification by recrystallization from ethanol solution. 1-Bromodecane, 1-bromododecane, 1-bromotetradecane, and 1-bromohexadecane were purchased from Tokyo Chemical Industry and employed without further purification. 1-Methylimidazole, 1-bromobutane, 1-bromooctane, 1-bromooctadecane, ethyl acetate, acetonitrile, and ethanol (HPLC grade) were purchased from Wako Pure Chemical Industries (Osaka, Japan), and 1-bromohexane and toluene were purchased from Nacalai Tesque (Kyoto, Japan); all these chemicals were used as supplied. An ion exchange resin, Amberlite® IRA-400 (chloride form), was purchased from Sigma-Aldrich (Tokyo, Japan) and used after anion exchange of chloride to hydroxide by immersion in a 1 mol L^{-1} aqueous NaOH solution.

Synthesis of [CnMim][Br] (n = 6–18)

All the N-substituted imidazolium salts used, 1-Cn-3-methylimidazolium bromide ([CnMim][Br]) (n = 6–18), were synthesized through N-alkylation/quaternization of 1-methylimidazole with different alkyl bromides according to the following method from the literature [19, 20]: 1-methylimidazole (0.10 mol) was dissolved in toluene (50 mL) at ambient temperature (~25 °C), and alkyl bromide (0.15 mol) was added to the solution. The mixture was stirred at 65 °C for 24 h in a round-bottomed flask equipped with a reflux condenser under a dry N$_2$ atmosphere. The toluene solvent was removed by decantation (for n = 6 and 8) or evaporation (for n = 10–18), and the crude product was dissolved in acetonitrile and then dropped into ethyl
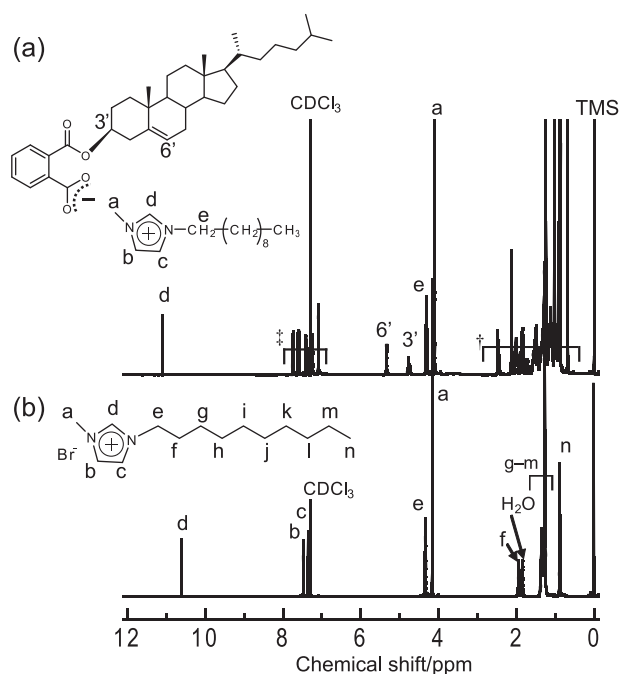

Fig. 1 Structural formulae of the cholesterol-based ionic complexes CHP (or CHS)/Cn-amine (studied previously [8–10]) and [CnMim][CHP] (targeted in the present paper)

Fig. 2 ^{1}H NMR spectra of **a** [C10Mim][CHP] and **b** [C10Mim][Br] in CDCl$_3$. Notations: †, proton signals in multitude from a steroid group of [CHP]$^-$ and f–n positions of [C10Mim]$^+$; ‡, proton signals in multitude from a benzene ring of [CHP]$^-$ and b and c positions of [C10Mim]$^+$. The peak integral values used for calculation of the complex composition (in **a**) are as follows: a, 42.12; e, 29.04; 3′, 14.49; 6′, 14.35

acetate under vigorous stirring. After the decanting of ethyl acetate, the remaining solvent was removed by heating the IL phase to 50 °C and stirring while on a vacuum line for 24 h. The salt products thus obtained were all identified as the respective [CnMim][Br] products by proton nuclear magnetic resonance (^{1}H NMR) measurements (see, e.g., the spectrum of [C10Mim][Br] given in Fig. 2b).

Preparation of [CnMim][CHP] complexes

Figure 3 shows an outline of the preparation route to the target complexes, [CnMim][CHP], from [CnMim][Br] and CHP as the starting materials.

By neutralizing an amino acid with imidazolium hydroxide, Fukumoto et al. [21] successfully prepared an amino acid IL. According to that method, we exchanged the bromide ion of the [CnMim][Br] salts ($n = 6$–18) with a hydroxide ion ([OH]) prior to complexation of the imidazolium cation with the carboxylate anion of CHP. Each [CnMim][Br] salt was dissolved in ethanol at a concentration of 2 wt% under stirring at room temperature (25 °C). Each [CnMim][Br]/ethanol solution thus prepared was passed through a column filled with hydroxide-exchanged Amberlite® IRA-400, and a series of 1-Cn-3-methylimidazolium hydroxide ([CnMim][OH])/ethanol solutions were

obtained. The absence of bromine in the latter solutions was confirmed by energy dispersive X-ray analysis. Then, a weighed amount of CHP was dissolved in each [CnMim][OH] solution under stirring at 25 °C for 24 h so that the mixture contained equimolar quantities of COO$^-$ from CHP and imidazolium cation. Each mixed solution was poured into a glass tray and dried at 25 °C. After further drying at 40 °C in vacuo for 24 h, [CnMim][CHP] complexes were obtained as a laminate product.
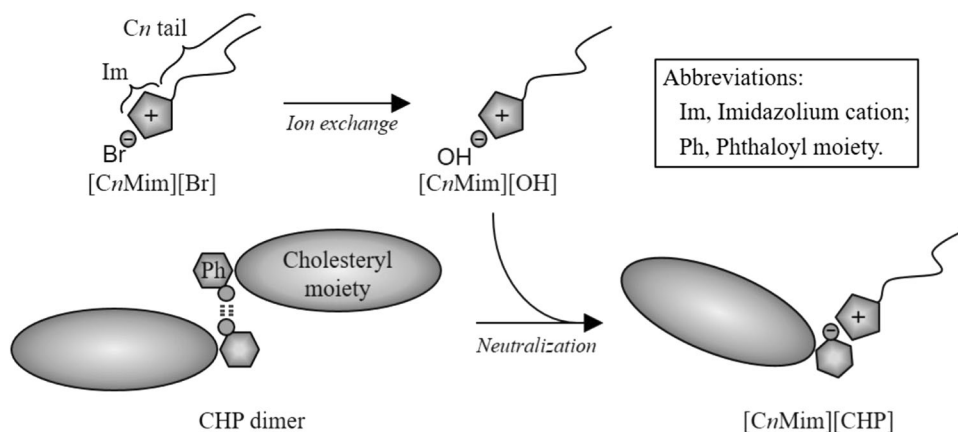
Measurements

Fourier transform infrared (FT-IR) spectra were measured with a Shimadzu IRPrestige-21 spectrometer (Shimadzu Corporation, Kyoto, Japan). All the spectra were recorded at 20 °C in absorption mode over a wavenumber range of 400–4000 cm^{-1} with a resolution of 4 cm^{-1} via the accumulation of 32 scans.

^{1}H NMR spectra (300 MHz) were recorded using a Varian INOVA 300 apparatus (Varian, Palo Alto, CA, USA). The measurement conditions were as follows: solvent, CDCl$_3$; solute concentration, 10 mg mL^{-1}; internal standard, tetramethylsilane; temperature, 20 °C; number of scans, 64.

Polarized optical microscopy (POM) was conducted by using an Olympus microscope (BX60F5, Olympus Corporation, Tokyo, Japan) equipped with a Mettler FP82HT/FP90 hot stage (Mettler Toledo, Tokyo, Japan). Samples were sandwiched between a slide and cover glass.

Differential scanning calorimetry (DSC) analyses were performed on a Seiko DSC 6200/EXSTER 6000 apparatus (Seiko Instruments, Chiba, Japan). Both the temperature and enthalpy readings were calibrated with an indium standard. A weighed amount of each sample (ca. 5 mg) was sealed in an aluminum pan. Thermograms were recorded at a scanning rate of 10 °C min^{-1} for both the heating and cooling scans. Measurements were conducted on all the prepared [CnMim][CHP] complexes to establish their respective phase transition patterns. The phase transition temperature and enthalpy were determined from the peak position and peak area, respectively, of the relevant endothermic or exothermic signal appearing in the thermogram. The T_g was evaluated by adopting the universal method proposed by Richardson and Savill [22] and Kimura et al. [23] (see Supplementary Information) to minimize the kinetic effects due to the scanning rate and the conditions of pretreating the sample. For this purpose, the usual DSC output data of the heat flow was converted into the corresponding relative enthalpy, H, and a plot of H against temperature was constructed. Next, two tangential lines were drawn on both sides of the glass transition region in the H versus temperature curve, and the temperature at the point of intersection was the T_g.

Fig. 3 Outline showing the preparation route to the [CnMim][CHP] samples ($n = 6$–18) from [CnMim][Br] and CHP

Another series of DSC measurements were carried out for selected complexes to evaluate the enthalpy relaxation following aging of their mesomorphic glass state. The sequence of procedures in the relaxation measurements is summarized below (see Fig. 4):

(1) Heating each original sample to a temperature higher than the mesophase–isotropic phase transition temperature, $T_{M–I}$, by ca. 15 °C.

(2) Cooling the isotropic sample at a rate of 10 °C min^{-1} to a temperature ($\approx T_g + 50$ °C) at which the sample assumes a mesomorphic fluid state.

(3) Quenching the mesomorphic sample at a rate of ~90 °C min^{-1} to an aging temperature, T_a ($< T_g$).

(4) Aging the glassy sample at T_a over a time period, t_a, in the DSC cell ($t_a < 1$ h) or in a thermoregulated incubator (NCB-3200, Tokyo Rikakikai, Tokyo, Japan) ($t_a \geq 1$ h).

(5) Quenching the aged sample from T_a to −60 °C.

(6) Heating the frozen sample at a rate of 10 °C min^{-1} from −60 °C to a temperature above the T_g.
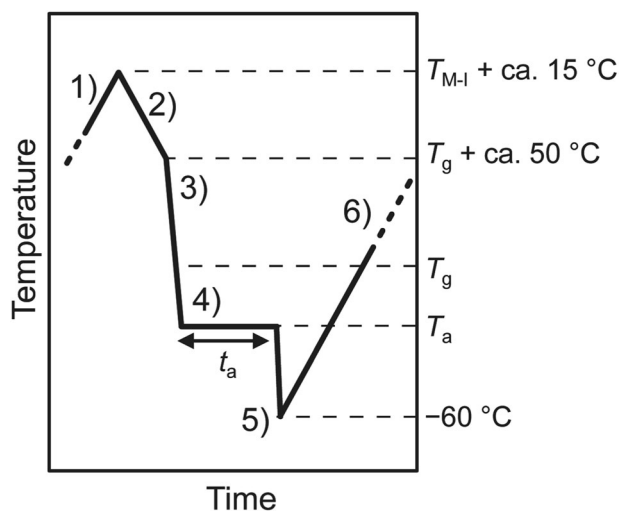

Fig. 4 Thermal program of the DSC measurements employed for the enthalpy relaxation experiments. $T_{M–I}$ mesophase–isotropic phase transition temperature, T_g glass transition temperature, T_a aging temperature, t_a aging time

Results and discussion

Formation of ionic complexes

Confirmation of ionic complex formation was obtained for the [CnMim][CHP] samples by ^{1}H NMR and FT-IR measurements. Figure 2 illustrates the ^{1}H NMR spectrum of [C10Mim][CHP] (part (a)) in comparison with that of [C10Mim][Br] (part (b)). The composition of this complex sample was evaluated as [C10Mim]/[CHP] = 0.99 using the peak intensities of signals **a** and **e** for the C10Mim component and those of signals **3′** and **6′** for the CHP component. In a similar manner of calculation, all the samples with various alkyl chain lengths ($n = 6$–18) showed a stoichiometric ratio of [CnMim]/[CHP] = 1.00 ± 0.04. Furthermore, it was observed that the chemical shift of one imidazolium proton (signal **d**) of [CnMim][CHP] was always higher by

ca. 0.5 ppm than that of the corresponding proton signal of [CnMim][Br]. In the two spectra given in Fig. 2, we find that this proton signal is located at 11.2 ppm for [C10Mim][CHP] and at 10.6 ppm for [C10Mim][Br]. A similar shift in the imidazolium proton signal toward lower magnetic fields has previously been noted for [CnMim][Ac] (Ac, CH$_3$COO$^-$) prepared from [CnMim][Br] [24, 25]. By comparison to this result, it may be inferred that the [CnMim][CHP] samples are 1:1 complex compounds linked through the formation of an imidazolium carboxylate salt.

Figure 5 displays the FT-IR spectra of CHP, [C10Mim][CHP], and [C10Mim][Br] as a reference. In the spectral data (a) of CHP itself, there appears a C = O stretching band at 1701 cm^{-1} and a C–O stretching band at 1310 cm^{-1}, both of which are associated with a carboxylic acid dimer. The other major bands observed at 1735 and 1255 cm^{-1} represent the ester linkage of cholesterol with phthalic acid in CHP. In the data (b) of [C10Mim][CHP], there are no

absorption signals for carboxylic acid. Instead, absorption bands signalizing carboxylate formation emerge at 1590 and 1370 cm^{-1} in the spectrum (b). These pieces of evidence support complete complexation between the two ionic constituents, [C10Mim]$^+$ and [CHP]$^-$. Similar FT-IR observations were made for the other [CnMim][CHP] samples. The formal features of the complexes may be

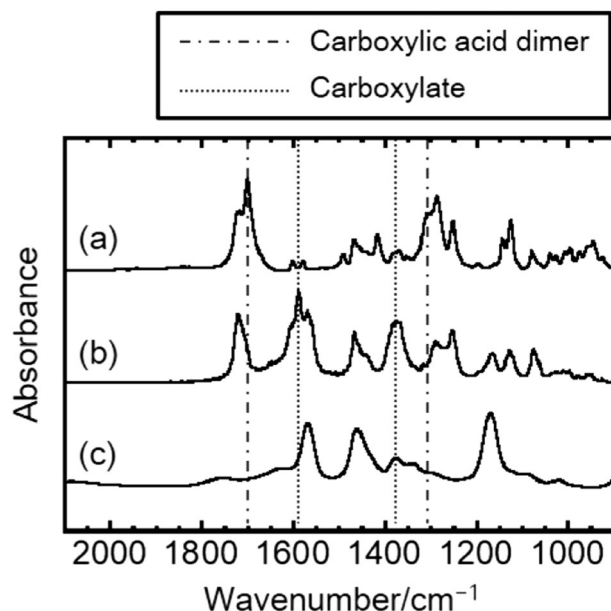**Fig. 5** FT-IR spectra of (**a**) CHP alone, (**b**) [C10Mim][CHP], and (**c**) [C10Mim][Br]. Spectra (**a**) and (**b**) were measured by the standard KBr pellet method. Spectrum (**c**) was recorded by a liquid-layer method in which the fluid sample was sandwiched between two KBr plates

likened to a fattened tadpole shape, as modeled in Fig. 3; the cholesteryl group possesses a Cn tail connected to a somewhat bulky joint comprising the phthaloyl and imidazolium moieties.

Thermal transition pattern

The thermal transition behavior of CHP was well established in earlier studies [8–10]. The known transition pattern was essentially reproduced in the present DSC measurements: upon heating, the original crystalline CHP obtained from ethanol solution melted at 169 °C and transformed into an isotropic liquid (I). When the molten CHP was cooled, the isotropic phase changed into a cholesteric mesophase (M$_{Ch}$) at ~85 °C. Upon continued cooling, the mesomorphic CHP vitrified at ca. 30 °C without crystallizing and retained a cholesteric planar texture. In the second heating scan, the anisotropic glass (G$_{Ch}$) changed again into the fluid mesophase at approximately 30 °C and then transformed into the isotropic liquid at ~92 °C. In the following cycles of cooling and heating, CHP showed the same enantiotropic phase behavior of I ↔ M$_{Ch}$ ↔ G$_{Ch}$ (see the first row of data listed in Table 1). It should be remarked here that the CHP molecules with a steroid mesogen dimerized through dual intermolecular hydrogen bonding between the COOH groups at their terminal ends (see Fig. 3), and this dimer is a structural unit involved in the observed phase behavior.

Similar DSC experiments were conducted for the tadpole-shaped [CnMim][CHP] complexes; all the samples were prepared as crystalline materials from ethanol solution.

Table 1 Thermal transition properties of CHP and the [CnMim][CHP] complexes

Sample	Pattern name	Phase transition pattern	T_g[a] (°C)	T_{M-I}[a] (°C)	ΔH_{M-I}[a] (kJ mol^{-1})
CHP alone[b]	—	G$_{Ch}$ ↔ M$_{Ch}$ ↔ I	25.8	91.4	3.3
[C6Mim][CHP]	A	G$_A$ ↔ I	13.9	—	—
[C8Mim][CHP]	A	G$_A$ ↔ I	7.8	—	—
[C10Mim][CHP]	B	G$_{Ch/Sm}$ ↔ M$_{Ch/Sm}$ ↔ M$_{Ch}$ ← I ↘ K ↗	10.4	81.1	— (1.0[c])
[C12Mim][CHP]	B	G$_{Ch/Sm}$ ↔ M$_{Ch/Sm}$ ← M$_{Ch}$ ↔ I ↘ K ↗	12.6	122.6	1.7 (1.8[c])
[C14Mim][CHP]	C	G$_{Sm}$ ↔ M$_{Sm}$ ↔ I	4.5	154.0	3.1 (3.1[c])
[C16Mim][CHP]	C	G$_{Sm}$ ↔ M$_{Sm}$ ↔ I	4.1	161.4	3.4 (3.4[c])
[C18Mim][CHP]	C	G$_{Sm}$ ↔ M$_{Sm}$ ↔ I	2.5	164.3	3.3 (3.6[c])

K crystal, *M* mesophase, *G* glassy state, *A* amorphous, *Ch* cholesteric, *Sm* smectic

[a]Estimated in the second heating scan
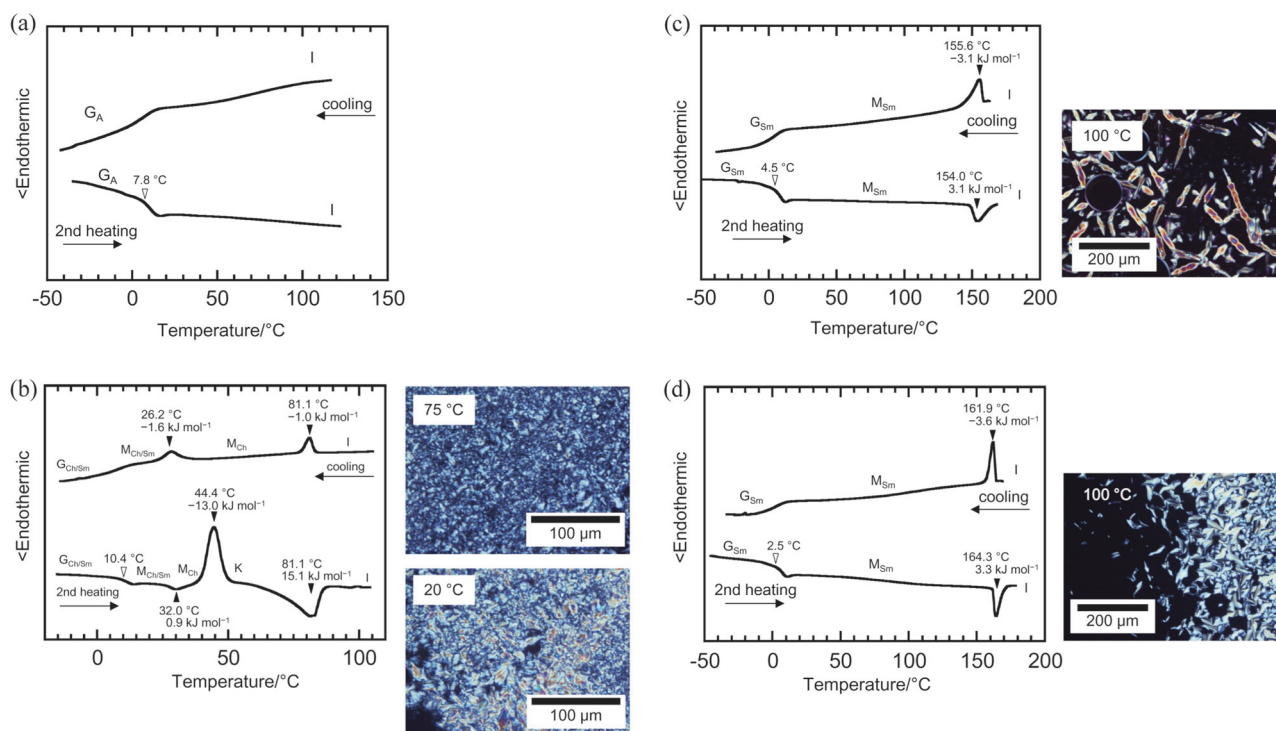
[b]Data quoted in ref. 8

[c]Estimated in the cooling scan

Fig. 6 DSC thermograms and POM images of selected [CnMim] [CHP] samples: **a** [C8Mim][CHP]; **b** [C10Mim][CHP]; **c** [C14Mim] [CHP]; **d** [C18Mim][CHP]. The thermograms were recorded at a scanning rate of 10 °C min^{-1} after isotropization of each sample by heating to a temperature >120 °C. The POM images were captured at various temperatures during the cooling process. In particular, the image in **c** was obtained by tilting the sample slide on the POM stage. K crystal, M mesophase, G glassy state, A amorphous, Ch cholesteric, Sm smectic

After isotropization of each sample by heating to a high temperature (>120 °C), the thermotropic phase behavior was evaluated in the subsequent cooling and heating cycles. The results are summarized in Table 1, and representative DSC data are compiled in Fig. 6. In general, we observed three patterns (A, B, and C) of phase transitions, which varied depending on the alkyl chain length (n) of [CnMim]$^+$.

Pattern A was observed for the thermal behavior of the complexes with n = 6 and 8. These samples exhibited only a glass transition (T_g < ca. 10 °C) without a phase transition accompanied by an exothermic or endothermic signal in the ordinary DSC cycles, as illustrated for [C8Mim][CHP] in Fig. 6a. Thus, these complexes repeated the transition behavior I ↔ G$_A$ (amorphous glass).

In pattern B, two mesomorphic phases appeared before the glass transition in the cooling process from the isotropic molten state, and consecutive crystallization and fusion processes occurred before isotropization in the heating process from the mesomorphic glass state. This pattern was observed for the thermal behavior of the complexes with n = 10 and 12. Fig. 6b illustrates the DSC thermograms of [C10Mim][CHP] together with supplementary POM photographic data. In the cooling scan, the isotropic melt (I) first transformed into a cholesteric mesophase (M$_{Ch}$) at 81 °

C, and then this phase partly changed into a smectic mesophase (M$_{Sm}$) at 26 °C followed by vitrification into a mesomorphic glass (G$_{Ch/Sm}$) at ca. 10 °C. This specification of the mesophases is supported by the transition enthalpy data (included in Fig. 6b, left) and by the POM observations. In Fig. 6b, right, the upper POM image shows a cholesteric planar texture, and the lower image exhibits a batonnet-like texture mixed with the planar one. In the subsequent heating scan, the anisotropic glass unfroze into a fluid mesophase (M$_{Ch/Sm}$) above 10 °C, and right after the transition of M$_{Ch/Sm}$ → M$_{Ch}$ at 32 °C, cold crystallization occurred at 40–50 °C from the M$_{Ch}$ state. Then, the resulting crystal (K) melted in a temperature range from 60 to 90 °C and ultimately transformed again into an isotropic fluid. Concerning [C12Mim][CHP], the pattern of "I → M$_{Ch}$ → M$_{Ch/Sm}$ → G$_{Ch/Sm}$" was also applicable to the cooling process; however, during heating, cold crystallization occurred at 45–65 °C from the M$_{Ch/Sm}$ state that was unfrozen above ~13 °C from the G$_{Ch/Sm}$ state. Following fusion at 70–90 °C of the formed crystal (K), the M$_{Ch}$ phase was restored and transformed into the isotropic melt at 123 °C.

Pattern C is classified as an enantiotropic pattern, I ↔ M$_{Sm}$ ↔ G$_{Sm}$, and was observed in the thermal behavior of the complexes with n = 14–18. Examples of the DSC

thermograms are given in Fig. 6c, d for [C14Mim][CHP] and [C18Mim][CHP], respectively. An isotropic liquid–mesophase transition (at >150 °C) and a single glass transition ($T_g \lesssim 5$ °C) were clearly observed in both the cooling and heating scans for these samples. The temperature range where the complexes were in an LC state was extremely wide. On examination by POM, a batonnet texture (Fig. 6c, right) or a fan-shaped texture (Fig. 6d, right) was observed for the mesomorphic fluid states. These optical images are characteristic of smectic-type liquid crystals. It was also observed that the complexes generally preferred a molecular arrangement in which they were oriented perpendicular rather than parallel to the surface of the glass slide in the mesomorphic state. This tendency may be ascribed to the homeotropic character of the Cn chain ($n \geq 14$) that served as a considerably long tail of the complexes.

From the survey of the results listed in Table 1, we can make the following remarks: (1) All the [CnMim][CHP] complexes except those with $n = 6$ and 8 form a mesophase and solidify into a mesomorphic glass (or LC glass) upon cooling. However, even the samples with $n = 6$ and 8 have the intrinsic ability to form a mesophase (according to their substantially slower kinetics), which was suggested by the microscopic observation of a feeble birefringent phase in the samples annealed at ~50 °C for more than 5 h. (2) The mesophase of [CnMim][CHP] tends to become more ordered with increasing length of the Cn chain (see ΔH_{M-I} data in Table 1); the molecular arrangement therein is dominantly cholesteric for $n = 10$ and 12 and smectic for $n = 14$–18. (3) The T_g of [CnMim][CHP] tends to decrease with increasing n and is always lower than that of CHP. In contrast, the phase transition temperature T_{M-I} increases with increasing n (≥ 10). In particular, the values (122–165 °C) for the complexes of $n \geq 12$ are extraordinarily high, well beyond that (92.0 °C) for CHP.

The Cn length dependence of the thermal behavior of [CnMim][CHP] was roughly similar to that examined formerly for CHP/Cn-amine complexes [8, 10]. In the latter system, however, the pattern of I ↔ M_{Sm} ↔ G_{Sm} (pattern C) was applicable to the complexes with Cn-amines of $n = 10$–18, and CHP/C8-amine provided a transition pattern of I ↔ M_{Ch} ↔ G_{Ch}, while CHP/C6-amine obeyed the pattern of I ↔ G_A (pattern A). Thus, the ordered phases, M_{Sm} and M_{Ch}, were formed from relatively shorter Cn chains compared with the situation in the [CnMim][CHP] system. Furthermore, the T_{M-I} values (ca. 85–100 °C) [8] observed for the CHP/Cn-amine samples of $n \geq 12$ were noticeably lower than those of the [CnMim][CHP] compounds with the same Cn lengths and comparable to that of CHP itself. The very high T_{M-I} values of the [CnMim][CHP] complexes might strongly reflect the thermotropic property of the N-substituted imidazolium IL, although there would be an

increase in the axial ratio of the mesogenic moiety of the complexes with the rigid imidazolium ring. According to the literature [14, 26–28], salts of [CnMim]$^+$ with longer alkyl chains ($n = 12$–18) are usually crystalline at room temperature and often exhibit an LC (smectic) phase in the molten state; for instance, the [CnMim][Br] complexes with $n \geq 12$ show transitions of K → M_{Sm} at or near 50 °C and M_{Sm} → I at temperatures much higher than 100 °C [27, 28].

Enthalpy relaxation of mesomorphic glasses

The physical aging of glassy materials, which generally occurs during their annealing at temperatures lower than the T_g, is interpreted as a spontaneous non-equilibrium phenomenon. More specifically, when a viscous fluid is vitrified below the T_g by cooling, the excess volume and enthalpy carried over into the solid should decrease with time toward the respective equilibrium values at the aging temperature. This behavior is commonly designated volume relaxation or enthalpy relaxation [29, 30] and is often accompanied by extensive changes in the mechanical properties and stability of the material [31–34]. In the present paper, our interest was focused on the enthalpy relaxation behavior of mesomorphic vitreous solids from a fundamental standpoint. The samples explored herein were the vitrified [CnMim][CHP] complexes with $n = 10$ and 18 that retained cholesteric and smectic mesomorphologies, respectively.
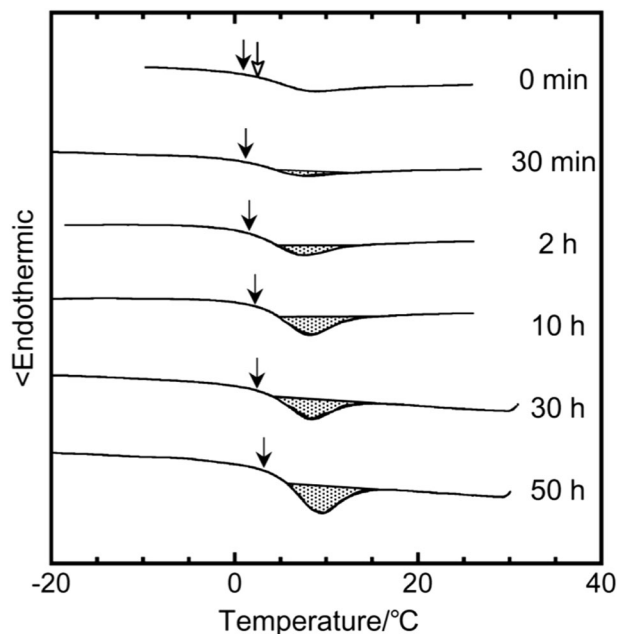

Fig. 7 DSC thermograms of the LC glass of [C18Mim][CHP] obtained after aging for the indicated length of time at −10 °C. The data were recorded in the heating scan at 10 °C min^{-1}. Solid arrows indicate the onset point of the glass transition, and the white arrow indicates the T_g position determined by a universal method proposed by Richardson and Savill [22] and Kimura et al. [23]

The enthalpy relaxation of glassy materials can be observed as an endothermic peak in their DSC thermograms just after the onset of the glass transition when the aged samples are heated. Fig. 7 illustrates the DSC thermograms obtained for the [C18Mim][CHP] LC glass that was aged for different time periods at −10 °C. The enthalpy ΔH can be evaluated from the endothermic peak area shaded in each thermogram. As expected, the area increased with increasing aging time, which was accompanied by a systematic shift in the peak position and in the onset point of the glass transition to higher temperatures. Fig. 8 illustrates the time evolution of ΔH for the glassy complex aged at various temperatures. The enthalpy rose rapidly with increasing time in the relatively early stage of aging and eventually leveled off and converged at the equilibrium enthalpy, ΔH_∞, the value of which became larger as the aging temperature was lowered. A similar trend in the dependence of ΔH on the aging time (t_a) and temperature (T_a) was observed for the [C10Mim][CHP] LC glass.

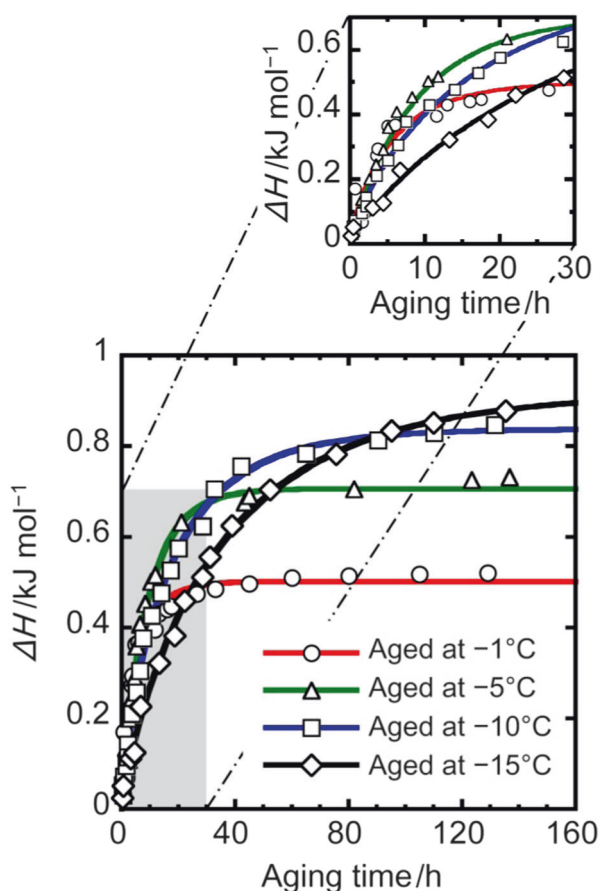Regression analysis of the ΔH versus t_a plots was made by employing the following KWW type of equation with a stretched exponential term: [35]

$$\Delta H = \Delta H_\infty \left[1 - \exp\left\{ -(t_a/\tau)^\beta \right\} \right], \qquad (1)$$

where τ is the enthalpy relaxation time and β is a non-exponential parameter ($0 < \beta \leq 1$) indicating the degree of distribution of the relaxation time. Table 2 lists the τ and β values determined by the best fitting of the ΔH data observed for the present complex glasses with $n = 10$ and 18.

In Fig. 9a, the logarithmic plot of τ against the reciprocal of the aging temperature (in K) is illustrated for the two glassy complexes. For both complexes, the plot provides good linearity, indicating the applicability of the Arrhenius equation:

$$\tau^{-1} = \tau_0^{-1} \exp[-E_a/(RT)], \qquad (2)$$

where E_a is the activation energy for the enthalpy relaxation process in the glassy state and τ_0^{-1} and R are the preexponential factor and the gas constant, respectively. Then, the energy E_a could be evaluated from the slope of each straight line of the plot. The result of the evaluation is listed in Table 2. Fig. 9b shows another plot of the ordinary logarithm of τ against the inverse of the T_g-reduced aging temperature for the mesomorphic glasses. According to Angell [36], the fragility of glassy materials is generally defined in the following way:

$$m = d \log \tau \, / \, d \left(T_g / T \right) |T = T_g, \qquad (3)$$

where m is the fragility index, and larger values of this index represent a higher fragility. Table 2 also lists the m data estimated from the slope of each Angell plot that gives a linear relationship in Fig. 9b.

Table 2 includes the results of a similar relaxation analysis performed for LC glasses of CHP and CHP/Cn-amine ($n = 10$, 16, 18) [9, 10]. In comparison with the previous results, the following remarks about the enthalpy relaxation data for the present complex glasses could be made:

(1) The parameter β for the [CnMim][CHP] glasses had a high value, situated at 0.90 and 0.84 on average for $n = 10$ and 18, respectively. In principle, the extreme of $\beta = 1$ means that a single (or unified) relaxation mode occurs, while when the distribution of the relaxation time is very broad due to concurrence of many relaxation modes in the aging process, β assumes a much smaller value that approaches zero. As seen from Table 2, the β values for the cholesterol-based LC glasses explored so far are all considerably larger than those (mostly 0.5–0.55) [37] reported for conventional amorphous polymers. Another observation is that the ionic complexes of CHP with Cn-amine and CnMim provided somewhat higher β values than (~0.7) the neat CHP (dimer) system.

(2) The relaxation times of the [CnMim][CHP] glasses were several to 40 times longer than those of the CHP/Cn-

Fig. 8 Time evolution of the enthalpy relaxation for the LC glass of [C18Mim][CHP] aged at different temperatures below the T_g

Table 2 Analytical results of the enthalpy relaxation for the LC glasses of CHP, [CnMim][CHP], and the comparable CHP/Cn-amine complexes

Sample	T_g (°C)	$T_g - T_a$ (°C)	ΔH_∞ (kJ mol^{-1})	τ (s)	$\ln \tau$ (s)	β	E_a (kJ mol^{-1})	m
CHP alone[a]	25.8	18.8	1.83	2.51×10^5	12.40	0.69	154	27
		10.8	1.31	3.34×10^4	10.40	0.74		
		5.8	1.21	1.00×10^4	9.22	0.78		
		2.8	1.02	7.94×10^3	8.97	0.70		
[C10Mim][CHP]	10.4	13.4	1.59	1.43×10^5	11.87	0.96	118	22
		10.4	1.44	7.41×10^4	11.21	0.95		
		7.4	1.27	4.04×10^4	10.61	0.87		
		3.4	1.03	2.19×10^4	9.99	0.80		
[C18Mim][CHP]	2.5	17.5	0.919	1.25×10^5	11.70	0.85	76	15
		12.5	0.887	6.06×10^4	11.01	0.82		
		7.5	0.842	3.16×10^4	10.36	0.84		
		3.5	0.502	1.96×10^4	9.88	0.84		
CHP/C10-amine[b]	18.7	16.7	1.69	9.17×10^4	11.4	0.87	94	17
		13.7	1.52	2.76×10^4	10.2	0.91		
		8.7	1.49	1.77×10^4	9.78	0.98		
		3.7	1.26	1.18×10^4	9.38	0.87		
CHP/C16-amine[a]	19.0	19.0	0.849	1.51×10^3	7.32	0.98	52	9
		14.0	0.604	9.53×10^2	6.86	0.92		
		10.0	0.408	7.41×10^2	6.61	0.90		
		7.0	0.262	5.61×10^2	6.33	0.84		
CHP/C18-amine[a]	20.0	25.5	0.990	2.37×10^3	7.77	1.00	47	8
		20.3	0.949	1.33×10^3	7.19	0.98		
		15.5	0.730	1.04×10^3	6.95	0.91		
		13.0	0.521	8.98×10^2	6.80	0.84		

[a] Data quoted in ref. 9

[b] Data quoted in ref. 10

amine glasses. The values of E_a estimated for the former glasses were higher than those estimated for the latter ones in samples having the same Cn length. With regard to the [CnMim][CHP] glasses, the bulkiness of the ionic junction involving an imidazolium moiety might lower the molecular mobility in the relaxation process. In both of the complex series, however, the E_a values were much lower than those (426–1070 kJ mol^{-1}) [38, 39] reported for poly(styrene).

(3) The fragility index, m, and E_a value for the [CnMim][CHP] glasses decreased with an increase in the Cn length, as was also the case for the CHP/Cn-amine glasses. The values for both series of ionic complexes were evidently lower than those for CHP itself. However, the estimations for [C10Mim][CHP] yielded somewhat larger m and E_a values, each of which approached the value for CHP, which may be attributable to an additional factor, that is, the prevalence of cholesteric ordering rather than smectic ordering. In any case, the Cn tail of the respective cationic components acted as a diluent solvent in the molecular assembly to promote cooperative motions. This motion should allow the glassy materials to be less fragile. Interestingly, the present result is in accordance with the general trend noted by Böhmer [40], in which the distribution of the relaxation time was considerably wider (i.e., β was lower), as the glassy material examined was more fragile.

Conclusion

Stoichiometric 1:1 ionic complexes, [CnMim][CHP] ($n =$ 6–18), were successfully prepared from ethanol solutions containing an equimolar mixture of CHP and [CnMim][OH]. The hydroxide was derived from [CnMim][Br] by exchange of the anion. The structural feature of the complexes is a fattened tadpole shape; the mesogenic cholesteryl group possesses a Cn tail connected to a bulky joint comprising phthaloyl and imidazolium moieties. The thermal properties related to the liquid crystallinity of the ionic complexes were investigated in comparison with the previous results obtained for a series of CHP/Cn-amine complexes.
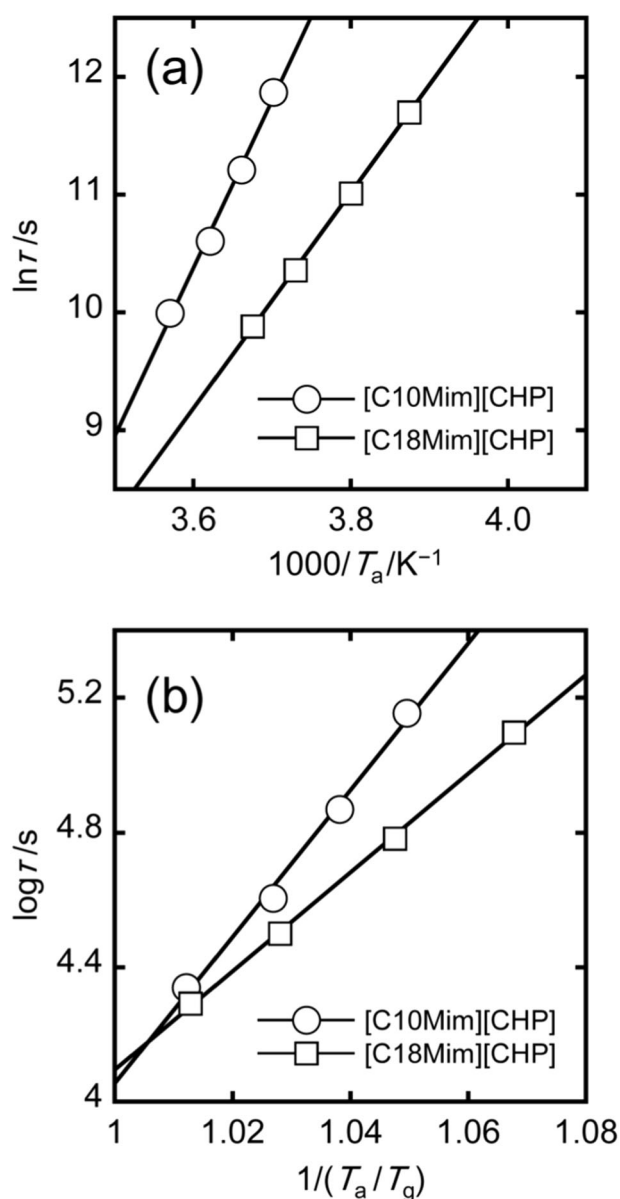
Fig. 9 a Arrhenius plots of the relaxation time against the reciprocal of the aging temperature and b Angell plots of the relaxation time against the inverse of the T_g-reduced aging temperature for the LC glasses of [C10Mim][CHP] and [C18Mim][CHP]

Concerning the transition behavior after isotropization, all the [CnMim][CHP] complexes except for the samples with $n = 6$ and 8 formed a mesophase and solidified into a mesomorphic glass upon cooling. The detected mesophase tended to become more ordered with increasing length of the Cn chain; the molecular arrangement therein was dominantly cholesteric for $n = 10$ and 12 and smectic for $n = 14–18$. The values of the isotropic transition point (i.e., $T_{M–I}$) observed for the samples with $n \geq 12$ were much higher than those for the CHP/Cn-amine complexes with the same ranges of Cn lengths. The marked elevation in the

$T_{M–I}$ values of the [CnMim][CHP] complexes can be interpreted as being due to the additional thermotropicity of the imidazolium salts with longer N-alkyl substituents.

For the mesomorphic glasses of [CnMim][CHP] ($n = 10$ and 18), the enthalpy relaxation behavior was monitored through the evolution in the endothermic DSC peak, and data analysis was performed in terms of the KWW type of stretched exponential function. Of significance was the confirmation of an extremely narrow distribution of relaxation times from the estimation of the exponent β close to unity. The activation energy, E_a, for the relaxation process and the fragility index, m, were also evaluated from the Arrhenius and Angell equations, respectively. The obtained E_a and m values were appreciably higher than those for the vitreous CHP/Cn-amine samples with the same Cn lengths. This result indicates that the bulkiness of the ionic junction comprising the imidazolium moiety lowered the molecular mobility in the relaxation process.

The present study should serve as a helpful guide for designing functional LC materials possessing vitrifiability. The thermal and optical properties of the cholesterol-based complexes may be varied not only by altering a component of the ionic junction but also by modifying the alkyl tail of the counter component. Meanwhile, the enthalpy relaxation analysis of the mesomorphic glasses provides useful information for understanding the physical aging of polymer glasses (involving both amorphous and LC glasses [39, 41]). The present results would still reflect the generic properties of low or medium molecular weight compounds. In this respect, we will be required to obtain further relaxation data using polymers having similar complex structures as the pendant group; this study is currently under way in our laboratory.

Compliance with ethical standards

Conflict of interest The authors declare that they have no conflict of interest.

References

1. Tsuji K, Sorai M, Seki S. New finding of glassy liquid crystal—a non-equilibrium state of cholesteryl hydrogen phthalate. Bull Chem Soc Jpn. 1971;44:1452–1452.
2. Wedler W, Demus D, Zaschke H, Mohr K, Schäfer W, Weissflog W. Vitrification in low-molecular-weight mesogenic compounds. J Mater Chem. 1991;1:347–56.
3. Tamaoki N. Cholesteric liquid crystals for color information technology. Adv Mater. 2001;13:1135–47.
4. Chen SH, Shi H, Conger BM, Mastrangelo JC, Tsutsui T. Novel vitrifiable liquid crystals as optical materials. Adv Mater. 1996;8:998–1001.

5. Fan FY, Culligan SW, Mastrangelo JC, Katsis D, Chen SH, Blanton TN. Novel glass-forming liquid crystals. 6. High-temperature glassy nematics. Chem Mater. 2001;13:4584–94.

6. Van De Witte P, Lub J. Optical components from a new vitrifying liquid crystal. Liq Cryst. 1999;26:1039–46.

7. Tamaoki N, Aoki Y, Moriyama M, Kidowaki M. Photochemical phase transition and molecular realignment of glass-forming liquid crystals containing cholesterol/azobenzene dimesogenic compounds. Chem Mater. 2003;15:719–26.

8. Kimura N, Takeshima N, Nishio Y, Suzuki H. Phase behavior of novel liquid-crystalline salts containing a cholesteryl group. Mol Cryst Liq Cryst. 1996;287:35–45.

9. Yoshio M, Miyashita Y, Nishio Y. Enthalpy relaxation behavior of liquid-crystalline glasses of an esterified cholesterol derivative and its complex salts with aliphatic amines. Mol Cryst Liq Cryst. 2001;357:27–42.

10. Nishio Y, Chiba R. Structural characteristics and novel functionalisation of liquid-crystalline polysaccharides and cholesterol derivatives. Ekisho. 2003;7:218–27.

11. Welton T. Room-temperature ionic liquids: solvents for synthesis and catalysis. Chem Rev. 1999;99:2071–83.

12. Hallett JP, Welton T. Room-temperature ionic liquids: solvents for synthesis and catalysis. 2. Chem Rev. 2011;111:3508–76.

13. Armand M, Endres F, MacFarlane DR, Ohno H, Scrosati B. Ionic-liquid materials for the electrochemical challenges of the future. Nat Mater. 2009;8:621–9.

14. Binnemans K. Ionic liquid crystals. Chem Rev. 2005;105:4148–204.

15. Axenov KV, Laschat S. Thermotropic ionic liquid crystals. Materials. 2011;4:206–59.

16. Goossens K, Lava K, Bielawski CW, Binnemans K. Ionic liquid crystals: versatile materials. Chem Rev. 2016;116:4643–807.

17. Yoshio M, Mukai T, Ohno H, Kato T. One-dimensional ion transport in self-organized columnar ionic liquids. J Am Chem Soc. 2004;126:994–5.

18. Shimura H, Yoshio M, Hoshino K, Mukai T, Ohno H, Kato T. Noncovalent approach to one-dimensional ion conductors: enhancement of ionic conductivities in nanostructured columnar liquid crystals. J Am Chem Soc. 2008;130:1759–65.

19. Bonhôte P, Dias A-P, Papageorgiou N, Kalyanasundaram K, Grätzel M. Hydrophobic, highly conductive ambient-temperature molten salts. Inorg Chem. 1996;35:1168–78.

20. Huddleston JG, Visser AE, Reichert WM, Willauer HD, Broker GA, Rogers RD. Characterization and comparison of hydrophilic and hydrophobic room temperature ionic liquids incorporating the imidazolium cation. Green Chem. 2001;3:156–64.

21. Fukumoto K, Yoshizawa M, Ohno H. Room temperature ionic liquids from 20 natural amino acids. J Am Chem Soc. 2005;127:2398–9.

22. Richardson MJ, Savill NG. Derivation of accurate glass transition temperatures by differential scanning calorimetry. Polymer (Guildf). 1975;16:753–7.

23. Kimura N, Aizawa K, Nishio Y, Suzuki H. Determination of glass transition temperature by differential scanning calorimetry. Kobunshi Ronbunshu. 1996;53:866–8.

24. Vitz J, Erdmenger T, Haensch C, Schubert US. Extended dissolution studies of cellulose in imidazolium based ionic liquids. Green Chem. 2009;11:417–24.

25. Matthews RP, Villar-Garcia IJ, Weber CC, Griffith J, Cameron F, Hallett JP, Hunt PA, Welton T. A structural investigation of ionic liquid mixtures. Phys Chem Chem Phys. 2016;18:8608–24.

26. Bowlas CJ, Bruce DW, Seddon KR. Liquid-crystalline ionic liquids. Chem. Commun. 1996; 1625–6.

27. Bradley AE, Hardacre C, Holbrey JD, Johnston S, McMath SEJ, Nieuwenhuyzen. Small-angle X-ray scattering studies of liquid crystalline 1-alkyl-3-methylimidazolium salts. Chem Mater. 2002;14:629–35.

28. Getsis A, Mudring A-V. Imidazolium based ionic liquid crystals: structure, photophysical and thermal behaviour of [C$_n$mim]Br·xH$_2$O (n=12, 14; x=0, 1). Cryst Res Technol. 2008;43:1187–96.

29. Weitz A, Wunderlich B. Thermal analysis and dilatometry of glasses formed under elevated pressure. J Polym Sci Polym Phys Ed. 1974;12:2473–91.

30. Cowie JMG, Ferguson R. Physical aging studies in poly(vinyl methyl ether). 1. Enthalpy Relaxation as a function of aging temperature. Macromolecules. 1989;22:2307–12.

31. Mininni RM, Moore RS, Flick JR, Petrie SEB. The effect of excess volume on molecular mobility and on the mode of failure of glassy poly(ethylene terephthalate). J Macromol Sci Part B. 1973;8:343–59.

32. Cavaille JY, Etienne S, Perez J, Monnerie L, Johari GP. Dynamic shear measurements of physical ageing and the memory effect in a polymer glass. Polymer (Guildf). 1986;27:686–92.

33. Bauwens-Crowet C, Bauwens J-C. Annealing of polycarbonate below the glass transition temperature up to equilibrium: a quantitative interpretation of enthalpy relaxation. Polymer (Guildf). 1986;27:709–13.

34. Struik LCE. Physical aging in amorphous polymers and other materials. Amsterdam, Netherland: Elsevier Scientific Pub. Co.; 1978.

35. Williams G, Watts DC. Non-symmetrical dielectric relaxation behaviour arising from a simple empirical decay function. Trans Faraday Soc. 1970;66:80–85.

36. Angell CA. Relaxation in liquids, polymers and plastic crystals—strong/fragile patterns and problems. J Non Cryst Solids. 1991;131-133:13–31.

37. Yoshida H. Enthalpy relaxation and fragility of amorphous polymers. Kobunshi Ronbunshu. 1996;53:874–6.

38. Yoshida H. Enthalpy relaxation of polymeric glasses. Netsu Sokutei. 1986;13:191–9.

39. Tanaka Y, Udagawa H. Structural relaxation of a side-chain type liquid crystalline polymer having longer spacer chain: analysis of enthalpy relaxation with an activation energy specrum. Kobunshi Ronbunshu. 2009;66:463–9.

40. Böhmer R. Non-linearity and non-exponentiality of primary relaxations. J Non Cryst Solids. 1994;172–174:628–34.

41. Tokita M, Funaoka S, Watanabe J. Study on smectic liquid crystal glass and isotropic liquid glass formed by thermotropic main-chain liquid crystal polyester. Macromolecules. 2004;37:9916–21.